

See discussions, stats, and author profiles for this publication at: <https://www.researchgate.net/publication/282133348>

Design for Fused Filament Fabrication Additive Manufacturing

Conference Paper · August 2015

DOI: 10.1115/DETC2015-46355

CITATIONS

32

READS

5,788

3 authors:



John Steuben

United States Naval Research Laboratory

94 PUBLICATIONS 904 CITATIONS

SEE PROFILE



Douglas Lee Van Bossuyt

Naval Postgraduate School

135 PUBLICATIONS 936 CITATIONS

SEE PROFILE



Cameron J. Turner

Clemson University

118 PUBLICATIONS 588 CITATIONS

SEE PROFILE

DETC2015-46355

DESIGN FOR FUSED FILAMENT FABRICATION ADDITIVE MANUFACTURING

John Steuben

Post Doctoral Research Associate
Department of Mechanical Engineering
Colorado School of Mines
Golden, CO 80401, USA
Email: jsteuben@mines.edu

Douglas L. Van Bossuyt*

Assistant Professor
Department of Mechanical Engineering
Colorado School of Mines
Golden, CO 80401, USA
Email: dvanboss@mines.edu

Cameron Turner

Assistant Professor
Department of Mechanical Engineering
Colorado School of Mines
Golden, CO 80401, USA
Email: cturner@mines.edu

ABSTRACT

In this paper, we explore the topic of Fused Filament Fabrication (FFF) 3D-printing. This is a low-cost additive manufacturing technology which is typically embodied in consumer-grade desktop 3D printers capable of producing useful parts, structures, and mechanical assemblies. The primary goal of our investigation is to produce an understanding of this process which can be employed to produce high-quality, functional engineered parts and prototypes. By developing this understanding, we create a resource which may be turned to by both researchers in the field of manufacturing science, and industrial professionals who are either considering the use of FFF-enabled technologies such as 3D printing, or those who have already entered production and are optimizing their fabrication process. In order to paint a cohesive picture for these readers, we examine several topic areas. We begin with an overview of the FFF process, its key hardware and software components, and the interrelationships between these components and the designer. With this basis, we then proceed to outline a set of design principles which facilitate the production of high quality printed parts, and discuss the selection of appropriate materials. Following naturally from this, we turn to the question of feedstock materials for FFF, and give advice for their selection and use. We then turn to the subject of the as-printed properties of FFF parts and the strong non-isotropic response that they exhibit. We discuss the

root causes of this behavior and means by which its deleterious effects may be mitigated. We conclude by discussing a mixed numerical/ experimental technique which we believe will enable the accurate characterization of FFF parts and structures, and greatly enhance the utility of this additive manufacturing technology. By formalizing and discussing these topics, we hope to motivate and enable the serious use of low-cost FFF 3D printing for both research and industrial applications.

1 INTRODUCTION

Fused Filament Fabrication (FFF), also referred to as Fused Deposition Modeling (FDM)¹, is an increasingly commonplace additive manufacturing technology [1]. In this paper we study the subject of design for manufacturing using the FFF process. We focus on the most common embodiment of this technology: low-cost consumer-grade desktop “3D-printers,” such as that illustrated in Figure 1. Multiple systems for this market have been developed [2-4].

The primary intent of this study is to develop a guide for the use of FFF for the production of engineered components in fields such as prototype, customized, or high-mix-low-volume manufacturing. This guide is largely geared to the needs of manufacturing science researchers and industrial engineers who are considering or have already adopted the use of FFF technology. We also explore the FFF process in detail, and develop an under-

*Address all correspondence to this author. Equally-shared corresponding authorship with Cameron Turner.

¹“Fused Deposition Modeling” and “FD” ©Stratsys Inc.
Copyright © 2015 by ASME

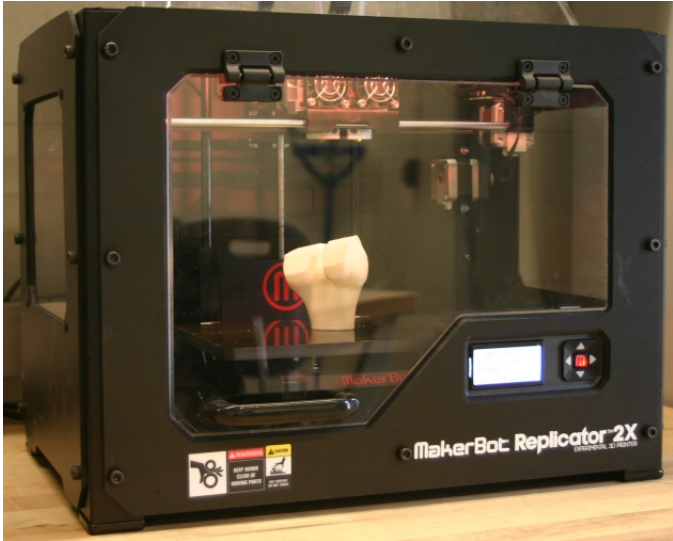


FIGURE 1. A typical desktop 3D printer which employs FFF.

standing of this technology which will enable the manufacture of high-quality components with minimum cost and waste. To do so, we examine several facets of fused filament fabrication.

1.1 Organization

We begin, in Section 2, by describing the FFF process as hardware and software components. The relationships between these components (and the design engineer) are shown, and the critical parameters associated with these connections are outlined. To illustrate the importance of these parameters, and show how they may be tuned, we proceed in Section 3 to lay out a set of design principles which enable efficient and productive FFF manufacturing. Important considerations for maximizing part quality and minimizing print time, cost, scrap rate, and wasted material are given. This discussion also includes recommendations for improving the geometric accuracy of the parts produced. In Section 4, we supplement the guidelines of Section 3 with a discussion of the feedstock materials available for FFF, and the best practices for selecting and printing with these materials. A summary of useful data for the selection of feedstock materials for an intended application is given. Section 5 expands upon the material properties theme, by considering the sources and implications of complex non-isotropic behaviors in FFF-produced components. We explore the sources of this anisotropy, and provide design and production advice for mitigating its deleterious effects. Finally, a discussion of the difficulties associated with simulating the response of FFF-produced structures is presented in Section 6. We further propose a mixed experimental/numeric scheme for characterizing the “as-printed” properties of these materials. By exploring these topics we produce a guide to the

process of low-cost 3D printing which is of interest to both researchers and practicing engineers who are either exploring the field of additive manufacturing with this process, or those who are already practiced in the art and wish to improve their own processes. As recent studies have shown that this technology is economically viable for distributed manufacturing [5, 6], we believe that this guide will enable a broad spectrum of future research.

1.2 Specific Contributions

In this paper, we gather observations and data which may already be familiar to those practiced in FFF. However, much of this important information has gone unreported, is reported in scattered sources, or is only discussed informally. Compounding this, much of the available scientific literature focuses on other additive manufacturing processes such as selective laser sintering [7] or powder and binder systems [8]. We wish to unify the available body of knowledge into a document which is useful both to new practitioners in the field of additive manufacturing, and those who are already well-versed in the field.

Beside the collection of practices and data that are useful to the manufacturing science researcher or production engineer, in this paper we contribute to the fundamental understanding of the FFF process in several aspects. In particular: 1) We formalize a great deal of knowledge from the hobbyist and professional communities, which has been validated in our laboratory. 2) We identify key parameters of the FFF process, and tie them to good design practice. 3) We present the best practices which we have found for 3D printing with the most common FFF feedstock materials, as well as post-processing operations such as vapor smoothing which may be utilized to improve output quality. 4) We combine existing research on the anisotropy of FFF-produced components, with research into an additional source of anisotropy, in order to identify the origin of delamination and fracture failures in these components. This work is validated by numerical and physical experimentation. 5) We identify shortcomings in both design practices and computational tools for addressing the complex anisotropic response behavior, and outline what we believe to be a promising path to rectify this deficiency through future research. Through these collective discussions, we paint a clear picture of the current best practices for low-cost FFF-based 3D printing, and enable the use of this technology with minimal difficulty by a wide range of researchers and industrial professionals.

2 The FFF Process

Before we discuss the topic of design methodology for FFF, we must first review the nature of the process, and identify the critical parameters which control it. Mechanically speaking, the FFF process is straightforward as illustrated in Figure 2. A

three-axis motion system moves an extruder in x-y-z coordinates, while extruding a certain amount of material, according to a pre-specified motion plan or “toolpath.” The extruder accepts polymer feedstock in the form of a filament, typically one to three millimeters in diameter and drawn from a spool. A drive gear engages the filament, and forces it through a thermistor-regulated heating block and nozzle. This produces a strand of molten plastic which is deposited and subsequently cools in order to form the FFF part. This deposition is produced in layers, built one atop the next. The relative distance between the extruder nozzle and build plate is adjusted in a fixed increment between layers. For each layer, both outer perimeter loops and a rasterized infill are extruded. The layers forming the top or the bottom of the part, adjacent to this infill region are typically solid. The infill is typically a sparse pattern in the areas of layers which correspond to the interior of the part. The FFF process is discussed in greater detail in [1]. Further review of common 3D printers employing the FFF process is given in [2-4].

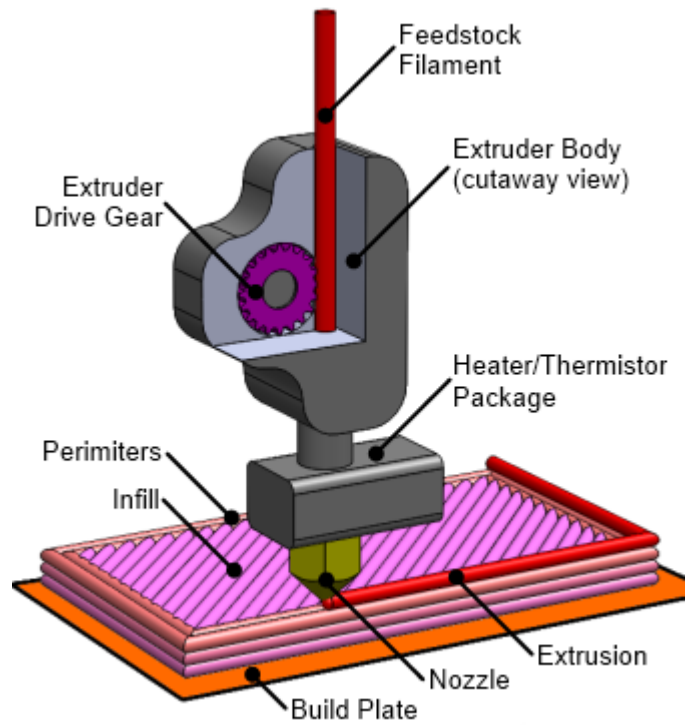


FIGURE 2. Illustration of the basic hardware setup for FFF 3D printing.

2.1 FFF Software Toolchain

Generally, the mechanical aspects of FFF are handled automatically by the printer hardware and firmware. It is therefore the generation a suitable toolpath which allows the production of parts in an efficient and timely manner. The software toolchain which is used to produce these toolpaths is diagrammed in Figure 3. The primary stages are (a) the generation of a 3D model from parametric engineering geometry such as a computer-aided drawing and/or imported 3D scan geometry, (b) converting the 3D model to a tetrahedral mesh file, almost universally implemented in stereolithography (STL) format, (c) splitting the tetrahedral mesh into layers and producing the toolpath using a program known as a “slicer,” and (d) using a piece of machine-control software to forward the toolpath to the printer itself, which then produces the part. This process is largely analogous to that used for industrial computer numeric control (CNC) machinery. The process of slicing, which is particularly complex, is covered in depth in [9-14]. Figure 4 demonstrates the full sequence of steps on a sample component.

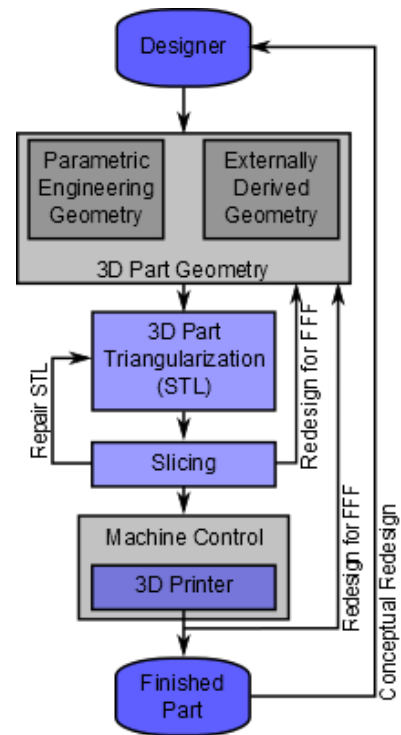


FIGURE 3. The FFF process, broken down into stages. Typically each stage takes the form of a separate software tool.

The process of Figure 3 includes several connections which indicate points at which iterative adjustment of the design may occur. These are not comprehensive, but indicate what we find

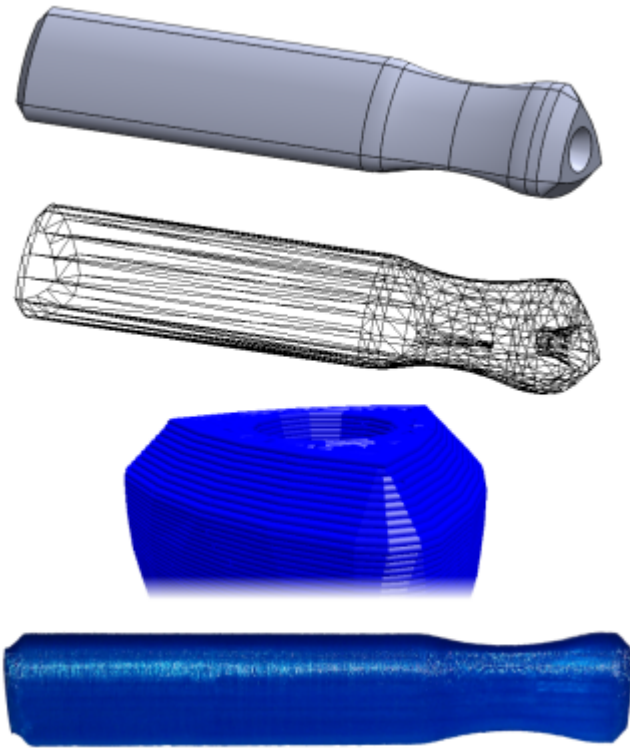


FIGURE 4. The stages of toolpath generation, from top to bottom: 3D part geometry, tetrahedral mesh, close view of toolpath produced by slicer, and finished product. Note that the part is rotated 90°.

to be the primary areas where designs must be adjusted to produce good results. Typically, the tetrahedral model will contain a very large number of facets, and it is difficult to manually check for the presence of errors. The better approach is to proceed to the slicing step, and observe if issues arise in the toolpath generation. The STL file input into the slicer must be a manifold “watertight” shell, and free of degenerate faces. Some Computer Aided Design (CAD) packages produce STL files containing degenerate facets or other errors. In this case, a software utility must be used to repair the STL file, such as those described in [15,16]. Additionally, the slicer may reveal issues which require correction by the designer. These issues may include thin features which the slicer may “miss” or cases where support material is difficult or impossible to remove. Information on preventing or rectifying these issues is discussed in Section 3. Other issues may be observed after the printing process is completed, and may require either redesign of the part to facilitate FFF, or a complete problem reformulation in order to achieve acceptable 3D printed parts. Methods for reformulating and designing parts for 3D printing are provided in Section 3.

2.2 Important FFF Parameters

The steps which follow the generation of the 3D model in Figure 3 rely on a number of important parameters. These are outlined and broken down by component in Table 1, below. The items listed are not comprehensive, and may vary based on the particular hardware and software used, but cover what we have found to be the most important and often-adjusted parameters. The typical values listed are based on our experiences with low-cost 3D printing systems, and the more common feedstock materials. Other fabrication systems and materials may require significant deviation from the ranges given.

This section has shown that FFF is a complex multi-stage process, which is governed by a large number of parameters. The correct selection values for these parameters is crucial to the production of high-quality low-cost parts. In the next section we explore design principles for FFF, which may be used both to generate FFF-ready components, and to more precisely select values for these parameters.

3 Design for FFF (DF4)

One of the great strengths of FFF and other 3D printing technologies is that they do not impose extensive design-for-manufacturing requirements, and enable the manufacture of parts which are difficult, expensive, or impossible to produce by conventional means. Examples of such parts are given in [17-20]. However, there are several design practices which may be observed in order to produce parts using FFF in a time and cost-effective fashion, especially for applications such as low-volume manufacturing. In the following section, we outline several of these practices which we have found to be most helpful, and which give insight into the tuning of the parameters listed in the prior section.

3.1 Part Orientation & Geometry

The layered nature of FFF, along with the physics of molten plastic extrusion place several limitations on the geometry which may be 3D printed. Chief amongst these are:

- The part must feature a planar surface which will be adhered to the build plate during printing. This planar surface must be of sufficient size (typically greater than 1cm^2) in order to remain adhered to the build plate for the duration of the printing process. If this is not possible the part should be printed atop a “raft” structure of sufficient area.
- The part should not exhibit geometric overhangs greater than a critical angle α , typically 45-60° from vertical. Such overhanging geometry necessitates the use of support material, as discussed in the next section.
- The part should be designed to carry major mechanical loads in the plane parallel to the build plate. Large out-of-plane

TABLE 1. Important parameters in the FFF process.

Parameter	Description	Typical Value
<i>Tetrahedralization</i>		
Max. Linear Deviation	Maximum distance between tetrahedral surface and original model.	0.03-0.1 mm
Max. Angular Deviation	Maximum angle between normal vectors of adjacent facets.	5-30°
<i>Slicing</i>		
Layer Thickness	Thickness of each layer of the FFF part.	0.05-0.3mm
Extrusion Width	Width of the plastic extrusion from the nozzle. Different widths may be specified for infill and perimeters.	0.1-0.4mm
Infill Density	Relative density from 0 (totally hollow object) to 1 (totally solid object).	0-1
Infill Orientation	Orientation of the infill pattern relative to the x-axis of the 3D printer.	0-90°
Infill Pattern	Pattern by which infill is produced. Rectilinear and hexagonal grids are most common.	–
Perimeter Loop Number	The number of perimeter loops produced (see Figure 3).	1-4
Perimeter Loop Ordering	Binary decision to print perimeters from innermost to outermost, or vice-versa.	–
Support Density	The relative density of the support material (again from 0/none to 1/solid).	0-0.3
Support Orientation	Orientation of the support material relative to the x-axis of the 3D printer	0-90°
Support Pattern	Pattern by which infill is produced. Rectilinear grids are most common.	–
<i>Printing</i>		
Movement Velocity	Rate at which to move the extruder head during plastic deposition. Separate rates may be specified for different extrusion types.	25-100 mm/s
Extruder Temperature	Temperature of the extrusion process	190-250 °C
Build Plate Temperature	Temperature of the build surface	0-140 °C
Cooling Power	Power applied to the cooling fans in order to solidify the extrusion.	0-100 %

loads promote delamination failures between the build layers due to the anisotropic material response characteristics, which are discussed in Section 5.

- The use of an “inverted frustum” design concept, as shown in Figure 5, can be used to accommodate these limitations. Effectively, the part should be located entirely within an inverted frustum of angle α , with a sufficient area on the bottom face to prevent part detachment from the build surface.

The topic of part orientation is covered in detail by [21-24], with extensive analyses. Even if the part is built within a frustum as described, there may still be local areas which require support material (e.g. some portions of the bracket in Figure 5). The next section covers the topic of generating support material.

3.2 Support Material

Unlike other processes such as selective sintering, FFF 3D printing requires the use of support material in order to produce overhanging structures such as the example shown in Figure 6. FFF printers which feature dual-extrusion heads may use one extruder to print the part and the other, loaded with a dissolvable material, to print the support structure. Materials such as polyvinyl alcohol (PVA) or high-impact polystyrene (HIPS) are frequently used in this capacity, as they are soluble in water or dipentene, respectively. More conventional printers with only one extruder are limited to producing “curtains” of support material which must be mechanically removed after the print. As a result, printing with a second support material tends to produce better accuracy and surface finish. However, in both cases

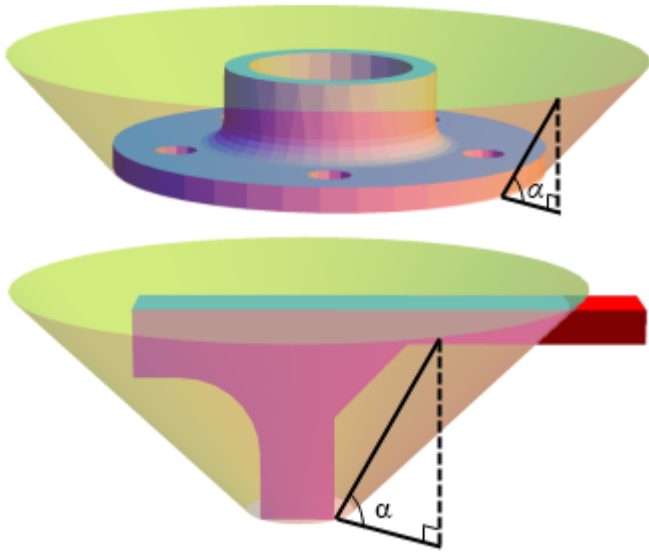


FIGURE 5. The inverted frustum design concept (with $\alpha = 45^\circ$) applied correctly on a wheel hub (top) and incorrectly on a bracket (bottom).

it is desirable to minimize the use of supports, as it represents additional material cost, post-processing cost, and machine time, which are not realized in the final product.

Examining Figure 6, it is clear that no reorientation of the (circularly symmetric) part will allow printing with less support material. This indicates that the part should either be printed in the shown orientation, or a redesign for FFF should take place. In this instance, if the studs were printed separately and press-fit in a secondary operation the part could be printed without support in the orientation shown in Figure 5. Given normal settings for support density and printer speed, this would result in a 37% savings in material consumption and a 39% decrease in print time based upon test prints of these configurations. These figures are computed by comparing the time estimates reported by a slicing program applied to both configurations using identical settings. This indicates that if parts cannot be printed without excessive support material, they should be split, printed in several parts, and assembled afterward.

Even more problematic are situations where overhanging areas which require support feature protruding bosses, as shown in Figure 7. This creates a situation where, for several layers, the boss will be printed atop the support material with no connection to the main part body. This causes very poor positional accuracy of the boss feature relative to the main part body, and a poor part finish on the bottom part of the boss. In cases where reorienting or splitting the part is impossible, the designer should model a support column and disable the automatic generation of support in the slicer. This is demonstrated in the bottom portion of Figure

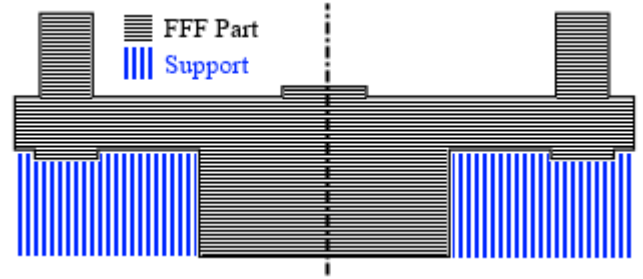


FIGURE 6. Example of areas requiring support material. A cross section of the wheel hub from Figure 5, with the addition of protruding studs, is shown.

7.

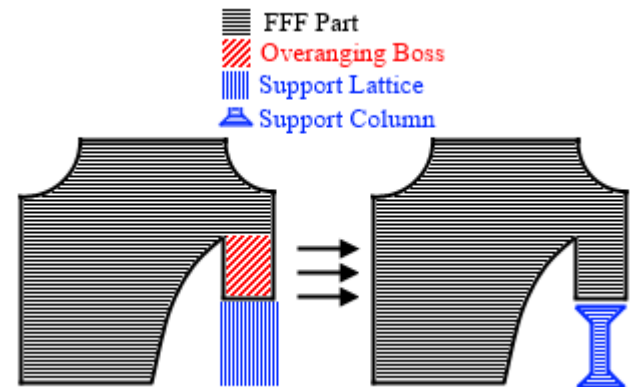


FIGURE 7. Overhanging features requiring support. It is advisable to provide a solid support column to accurately locate the overhanging boss.

A final difficulty concerning support material involves the concavity of regions where support is generated. If the support is not printed from soluble material it must be mechanically removed. Producing an acceptable surface finish usually requires finishing with a file or other abrasive. If the support material had been generated beneath a small concave area this process may be difficult or impossible. Additionally, if support material is placed on top of a portion of the printed part, it will be more difficult to remove. These conditions are outlined in Figure 8.

In summary, the best design practices regarding support material are:

- Always consider reorienting or splitting the part in order to reduce or eliminate the usage of support material.

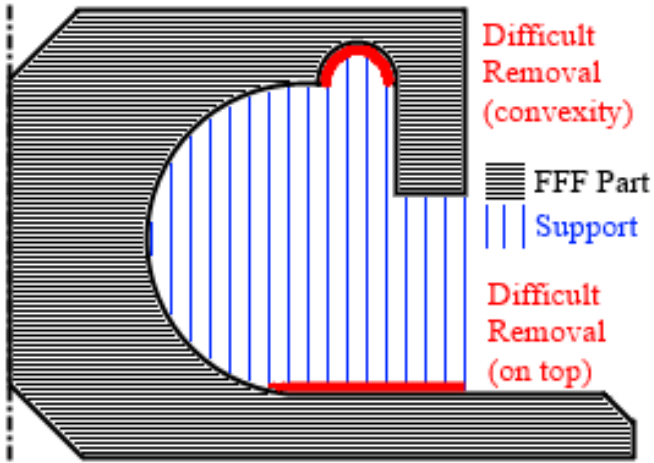


FIGURE 8. Areas where support material may be particularly difficult to remove from a revolved part.

- Include pillar supports in order to accurately locate overhanging boss features.
- Avoid the generation of support material in areas where it will be difficult to remove (e.g. small concave regions).
- Support material should be generated at an angle orthogonal to the long axis of the region which it supports
- The support lattice should be spaced by approximately $\frac{1}{2}$ the size of the smallest supported feature, or 3mm, whichever is smaller.

3.3 Infill

In order to minimize the use of material FFF, parts are usually built from a solid outer perimeter shell, but feature a sparse interior infill pattern on the interior. The perimeter and infill are generated automatically by the slicer program. Several of the parameters given in Table 1 can be adjusted to produce satisfactory parts. As a rule, both the mechanical strength and production cost will increase proportionally to the infill density. We recommend an infill density of 0.1-0.125 for purely cosmetic parts, and 0.125-0.2 for light-duty parts (dust guards, cable guides, etc). For more heavily-stressed components such as mechanical linkages or gears, a higher density in the range of 0.25-0.5 is recommended. For components such as wrenches or long levers, a density of 1.0 (completely solid) has produced acceptable results.

The infill is commonly constructed in either rectilinear or hexagonal patterns, as shown in Figure 9.

Generally we prefer the use of rectilinear infill for two reasons. First, a rectilinear infill is simpler to compute, results in a smaller toolpath file, and requires slightly less printing time. For the comparison shown in Figure 9 the linear infill is 3% faster to



FIGURE 9. Hexagonal (top) compared to rectilinear (bottom) infill. Note both the outer perimeters and the perimeters around the interior holes.

print, as computed by slicing the same part twice, varying only the pattern, and comparing estimated print times. Second, a rectilinear infill allows the relative orientation of the infill strands to be adjusted along with the mechanical properties of the part. The orthogonal configuration shown in Figure 9 is not mandatory. Alternate configurations enable the adjustment of mechanical properties so as to reduce anisotropic material behaviors, as discussed in Section 5.

3.4 Surface Finish

Achieving a fine surface finish is highly desirable for most 3D printing processes, but achieving a consistently good surface finish using FFF is difficult. There are a multitude of factors which contribute to this difficulty, such as the layered nature of the part, the inherent unpredictability of the molten or semi-molten plastic flow, and drooping or sagging in overhanging regions. In this section we focus on design measures which can be used to improve surface finish. In Section 4 we discuss the material-specific thermal management issues which can further improve surface finish.

One of the key determinants of surface finish is layer thickness, as illustrated in Figure 10. Given the idealized geometry shown in the top portion of Figure 10, it is clear that $d_1 = \sin(\alpha')$, $d_2 = \frac{t}{2}$, and thus the surface deviation (d) is approximated by $d = d_1 + d_2 = (\frac{t}{2})(1 + \sin(\alpha'))$. This relationship illustrates that both the layer thickness (t) and the slope of the local geometry (α') affect the surface finish on the “sides” of the model. The lower portion of the figure illustrates the finish on the “top” surface of the part, and shows that the extrusion width does not play a major role and that the top surface deviation (d') is approximately given by $d' = \frac{t}{2}$.

The strong dependence on layer thickness is clear, and by reducing this dimension to 0.1 mm or less a very fine surface

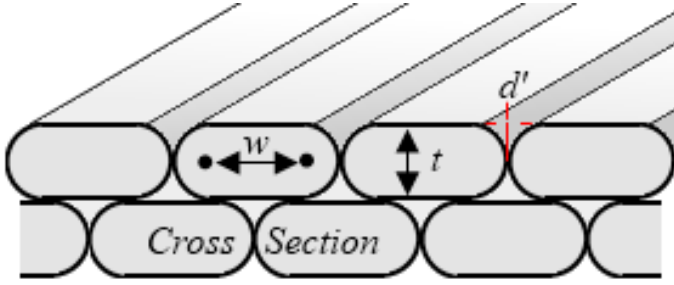


FIGURE 10. Illustration of surface deviation in an idealized FFF model.

finish can be obtained. Unfortunately, print time increases in a fashion inversely proportional to layer thickness. For all practical purposes this is an exact correspondence, e.g. printing at double the layer thickness will halve print time. Typically the lower limit of layer thickness is dictated by the mechanical accuracy of the 3D printers motion system, and the upper bound is equal to the extruder nozzle diameter.

The idealized model shown in Figure 10 does not illustrate several of the other factors associated with poor surface finish. The use of support material, for instance, will reduce the surface finish quality of the areas to which the support material is attached. Another common problem is “droop” where the outer perimeters of a layer are not supported properly by the layer(s) below and are drawn downwards by gravity before the molten extrusion can sufficiently solidify. Many of these effects can be mitigated, however, by the correct selection of properties for the perimeter loops which are given in Table 1. A few helpful observations include:

- Printing the perimeters from “outside” to “inside” produces better dimensional accuracy, but reversing the ordering produces better surface finish on overhanging surfaces.
- Usually 2-3 perimeters are sufficient to produce good dimensional accuracy and surface finish. For parts with excessively steep overhangs (or conversely, very gently sloping non-overhanging regions), more perimeters may be required.
- The outermost perimeter should be printed at a slower speed, roughly 50-75% the speed of other perimeters.
- Prior research has also shown that surface finish may be improved by optimizing the vertices of the STL file which is input to the slicer [25]. Further details concerning the generation of the STL file are given in the next section.

3.5 Generating the STL File

The conversion of a parametric solid model to a tetrahedral mesh is the final step of the design process for FFF, and should be approached with care. The mesh must consist of one or more

manifold surfaces with no gaps or holes. Non-manifold meshes typically cause errors and nonsensical toolpath generation during slicing. Most CAD packages support the direct export of manifold mesh files. A stereolithography STL file is almost always used, although research in other additive manufacturing fields has shown that specialized file formats may have some benefit [26]. Typically two tolerance parameters can be adjusted to define the fidelity of the mesh: maximum distance and angular deviation. If these tolerances are too large, the mesh will not adequately represent the underlying model; if the tolerances are too small, the mesh will be excessively large and require extensive time and computer resources to slice. The settings most commonly used in our work are:

- Fine models: Max Deviation = 0.025 mm, Max Angle = 5°
- Coarse models: Max Deviation = 0.1 mm, Max Angle = 20°
- Very fine models: the maximum deviation should be equal to the smallest feature which the FFF hardware can reproduce (determined experimentally). The maximum angle tolerance should be greater than 1°.

Regardless of the settings used, the output of the STL mesh should not exceed a few hundred megabytes in size (unless it corresponds to a very large model). Typically gigabyte sized STL files contain details that are far finer than the printing hardware can reproduce. These very fine features will increase the time required for slicing, and may cause surface finish problems during printing. An example of coarse, fine, and very fine meshes can be seen in Figure 11.

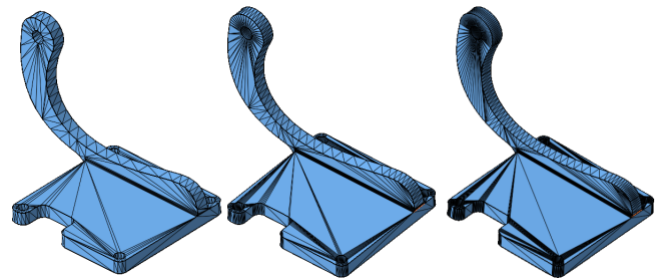


FIGURE 11. Coarse (left), fine (center), and very fine (right) meshes of a mounting bracket.

A final issue regarding meshing is that many CAD systems produce poor quality STL output files that may contain very high aspect-ratio facets, or other degenerate features. The use of remeshing software such as [15] to produce high-quality meshes is encouraged. Some extremely high-aspect ratio triangles can be seen in the fine and very fine portions of Figure 11.

The procedures and practices outlined in this section can be used to design parts which can be efficiently produced using FFF.

This discussion has primarily involved the geometry, surface finish, and representation of the part. Details and advice for the actual fabrication of such parts, particularly with respect to material selection and treatment, are given in the next section.

4 Material Selection

In the prior sections, we have discussed the topic of designing a part for efficient FFF production. Once this process has been completed, we must turn our attention to the actual production of such a design. The question of selecting an appropriate FFF feedstock material remains, as do subsequent questions regarding the best practices for low-cost 3D printing with these materials. In this section, we explore the properties of some of the most common feedstocks and offer both general and specific advice for their employment in inexpensive 3D printers. This discussion also includes further discussion of tuning the process parameters given in Table 1. The bulk properties of feedstock materials are a good place to begin this study. While the FFF process, particularly the bonding of layers, produces parts with ultimately different properties, the bulk properties can be useful for the selection of materials based on application or intended usage. In Table 2, we give aggregate data on the properties of four common materials used for FFF.

Of these materials, we have observed ABS and PLA to be the most common FFF feedstocks for low-cost desktop 3D printing applications, by a large margin. PLA is easier to print and produces a good surface finish, but ABS typically produces more durable parts. There are also a number of newer nylon polymers that have been developed for FFF, which have not yet been rigorously characterized. We discuss practices for successful printing for the materials in Table 2. There are also several general practices which apply to all of these materials which should be observed.

4.1 General Material Considerations

Among the materials frequently used in FFF, there are several common practices which should be observed. The properties (from Table 2) of any feedstock material vary considerably based on variations such as: manufacturer, trade name, or the presence of additives or colorants. It is therefore necessary to characterize the properties, especially the extrusion temperature, when using new materials. It is generally desirable to print at the highest temperature possible in order to improve bonding between layers. Printing a series of test specimens, starting at the minimum temperature from Table 2 and increasing the extruder temperature until the surface finish or mechanical accuracy of the specimen degrades, is the easiest way to dial in this parameter. Usually raw polymers, free of dyes or stabilizers, exhibits the best mechanical strength. Most of the feedstock polymers are also hygroscopic, and must be stored in a sealed container with

TABLE 2. Important parameters in the FFF process.

Property	Min.	Max.	Avg.	Units
<i>ABS Acrylonitrile Butadine Styrene [27]</i>				
Elastic Modulus	1.00	2.65	2.09	GPa
Tensile Yield Strength	13.0	65.0	41.5	MPa
Tensile Ultimate Strength	23.0	49.0	38.0	MPa
Extrusion Temperature	215	274	229	°C
Max. Service Temperature	60	100	85.2	°C
<i>PLA Polylactide / Polylactic Acid [28]</i>				
Elastic Modulus	0.23	13.8	3.63	GPa
Tensile Yield Strength	16.0	103.0	44.7	MPa
Tensile Ultimate Strength	16.0	114	49.3	MPa
Extrusion Temperature	171	220	201	°C
Max. Service Temperature	60	130	77.5	°C
<i>PET Polyethylene Terephthalate [29]</i>				
Elastic Modulus	1.83	5.20	3.45	GPa
Tensile Yield Strength	47.0	90.0	62.4	MPa
Tensile Ultimate Strength	22.0	155.0	72.8	MPa
Extrusion Temperature	120	295	252	°C
Max. Service Temperature	100	225	153	°C
<i>Polycarbonate [30]</i>				
Elastic Modulus	1.79	3.24	2.38	GPa
Tensile Yield Strength	58.6	70.0	63.7	MPa
Tensile Ultimate Strength	60.0	74.0	67.9	MPa
Extrusion Temperature	250	343	300	°C
Max. Service Temperature	115	135	124	°C

desiccant. Failure to do so results in steam formation in the extruder's hot zone, which causes radical degradation of the surface finish of the printed part.

It is of paramount importance to ensure that the build plate is parallel to the plane defined by the x and y-axes of the 3D printer. While some variation, on the order of $\frac{1}{2}$ the layer thickness, is tolerable, variation in the "bed leveling" reduces the geometric accuracy of parts produced and also dramatically reduces the adhesion of the first layer to the print bed. This leads to a high scrap rate if the printer is not routinely calibrated. While a feeler gauge can be used to level the bed, this process is iterative and time-consuming. We recommend the fabrication (using FFF) of a clamp or bracket which allows the attachment of a dial gage to the extruder body, such as the one shown in Figure 12. The gauge can then be installed, the bed leveled, and removed in much less time than leveling using feeler gages. Once the bed has been accurately leveled in this fashion, the slicer can be instructed to print the first layer at $\frac{1}{2}$ to $\frac{3}{4}$ the specified thickness, producing a thinner, wider extrusion which adheres more tightly to the build surface.

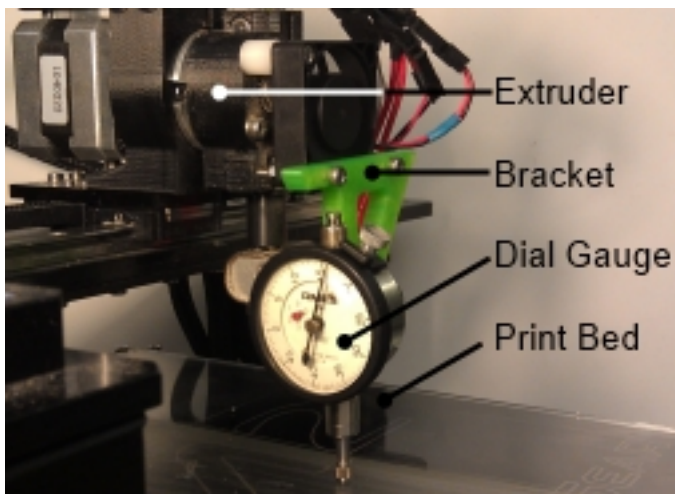


FIGURE 12. Illustration of the use of a dial gauge for bed leveling.

4.2 Printing with PLA

PLA is the easiest material to print using conventional FFF 3D printers, and exhibits good mechanical properties. It is comparatively rigid and tends to exhibit fracture and delamination failures long before yielding can occur. PLA can be printed without the use of a heated printbed. Materials such as acrylic polymer or borosilicate glass are commonly used to construct the printbed. Adhesion to the printbed can be improved, which

is especially helpful for large prints or those with limited contact areas, by using a heated printbed at 70C. PLA prints can be smoothed to erase layering artifacts by exposure to several solvents; the most commonly used are methyl ethyl ketone (MEK), ethyl acetate, and tetrahydrofuran (THF). Vapor smoothing can be employed by suspending the part on a scaffold within a container partially filled with solvent which is gently heated to produce vapor. An example of vapor smoothing is shown in Figure 13. Mechanical smoothing, using a brush to physically work solvent against a part, is also feasible. In both cases, care should be taken due to the flammable and/or toxic nature of the solvents used.



FIGURE 13. Bevel gears manufactured from PLA using FFF in the "as printed" state (at left), and after a 10-second exposure to ethyl acetate vapor at 115 °C (right).

4.3 Printing with ABS

ABS is somewhat more difficult to use for FFF as it typically exhibits a larger contraction upon cooling. This produces forces that tend to pull the edges of the part up from the build plate, which causes the entire part to detach before printing is finished. The use of a heated printbed is mandatory. A printbed temperature of 100-140 °C greatly improves adhesion. There are several surface treatments which can be applied to the printbed to further improve adhesion. The application of polyimide tape can greatly improve adhesion, but adds expense to the printing process as it requires frequent replacement. The application of a slurry of ABS (usually produced from printing scraps) dissolved in acetone which is allowed to evaporate produces an extremely strong bond to the printbed. A ratio of around 20:1 of acetone to ABS by weight is typical. High fractions of ABS produce an excessively strong bond which renders printed parts difficult to remove from the build plate. A 5:1 mixture of water to water-

based wood glue produces a reliable surface bond which we have found to be a good compromise between adhesion and easy part removal.

The volumetric contraction of ABS as it cools also makes it difficult to print large parts without a loss of geometric accuracy, or the formation of fractures in some cases. The use of a heated enclosure maintaining an air temperature of 70-100 °C greatly reduces this effect. ABS can be smoothed in the same manner as described for PLA, but an acetone solvent is most effective.

4.4 Printing with PET

PET is a lightweight material with excellent mechanical properties which can be used to manufacture high-durability mechanical parts using FFF. It is also produced in optically transparent grades which are useful for producing parts compatible with non-destructive testing regimes (e.g. food-safe components). Higher extrusion temperatures are favorable for promoting transparency; lower temperatures produce an opaque finish. PET is generally easier to print than ABS and does not require a heated bed. Sufficient adhesion can be achieved by applying blue “painters tape” to the build plate. PET can also be smoothed using MEK or ethyl acetate. Care must be taken due to the toxic and/or flammable properties of these solvents.

4.5 Printing with Polycarbonate

Like PET, polycarbonate can be used to print high-durability parts. Anecdotal evidence [31] indicates that it has successfully been used to print high-speed rotating components for industrial machinery. The downside of this material is that it requires higher extrusion temperatures than many commodity 3D printers are capable of producing. Printbed adhesion is most easily achieved by using a polyimide tape coating. As with PET, higher temperatures promote transparency in the printed part, and in the case of polycarbonate higher temperatures are required to prevent the formation of residual stresses. We have not conducted experiments regarding the smoothing of polycarbonate parts, but in theory any applicable solvent such as dichloromethane may be used. Generally, the solvents appropriate for use in smoothing polycarbonate are toxic, and care must be taken in their use. The discussion in this section is limited to the bulk properties of common FFF feedstock materials, and outlines their proper use along with advice for their employment in 3D printing. In the next section we concern ourselves with the “as printed” properties of structures produced from these feedstocks, and the complex responses that they exhibit.

5 Anisotropy in FFF Structures

In many applications, objects produced using FFF need only be the correct shape, and no specific mechanical properties are required. Architectural models [32], simple toys, and artistic

sculptures [33] are examples of this sort of application; inexpensive desktop 3D printers have been used with great success in these fields. In these cases, the design and printing practices outlined in the previous sections can be used without modification. However, there is a strong desire in both hobbyist and professional communities to produce serviceable mechanical and structural parts using FFF on inexpensive commodity hardware. These applications require printed parts which exhibit sufficient strength, stiffness, wear resistance, or other properties. It is therefore important to be able to estimate the mechanical properties of a FFF-produced part before it is printed in order to augment and inform the design process outlined previously. Failure to estimate mechanical properties accurately reduces the design process to a trial-and-error exercise which results in wasted production time and material. Unfortunately, the complex geometry and anisotropic constitutive response of FFF-produced parts complicates this process greatly.

5.1 Sources of Anisotropic Behavior

The anisotropic behavior of FFF-produced parts has previously been observed and remarked upon [34-36]. This anisotropy results from:

1. The pattern and orientation of the sparse infill used [35].
2. The temperature-dependant nature of the bonding between successively extruded polymer filaments.

Anisotropy due to the sparse infill is caused by the inability of the internal air voids which are formed to support mechanical loads. Consider the case of rectilinear infill as shown in Figure 9: each layer is printed with strands oriented in the same direction, and successive layers create the crosshatched pattern seen. This implies that any given layer is relatively stiff along the direction of the extruded strands, and relatively compliant in the orthogonal direction. Stacking these layers results in orthotropic behavior such as that typically seen in polymer-matrix composites [37].

The second source of anisotropy has been explored to a lesser extent. Generally, the bonding of molten polymers is controlled by a diffusion process [38, 39] which is dependent on the temperature and contact pressure in the bonding zone, as well as the time allowed for diffusion to occur. Given that bonding in the FFF process occurs at ambient pressure, it appears that printing speed is the primary factor in developing bond strength. However, temperature difference also plays a major role [40]. If the extruder is laying down molten polymer against freshly deposited substrate which is still near the extrusion temperature, the local temperature will be high, thus promoting strong bonding. However if the extruder is depositing plastic against a substrate which has been allowed to cool, such as when beginning a new layer of a large part, the bonding temperature will be comparatively low and result the resulting bonds will be far weaker.

The weak bonding between layers produced by thermal effects is compounded by the orthotropic material properties produced by the infill. The alternating stiffness and compliance along a given axis in each layer produce stress concentrations between the layers. We conducted a simple numerical and physical experimental pair to demonstrate this phenomenon. An ANSYS finite-element model was used to model an orthotropic material specimen of double-notch geometry with properties corresponding to raw ABS polymer. A torsion load was applied in order to produce the theorized stress concentration. The physical specimen, when similar loads were applied, exhibited a delamination/fracture failure originating in the same location, and following the same path, as predicted in the numeric model. These results are shown in Figure 14. The geometry of the simulated model differs from that of the physical specimen as the mechanically gripped areas were presumed to be completely rigid, and not simulated.

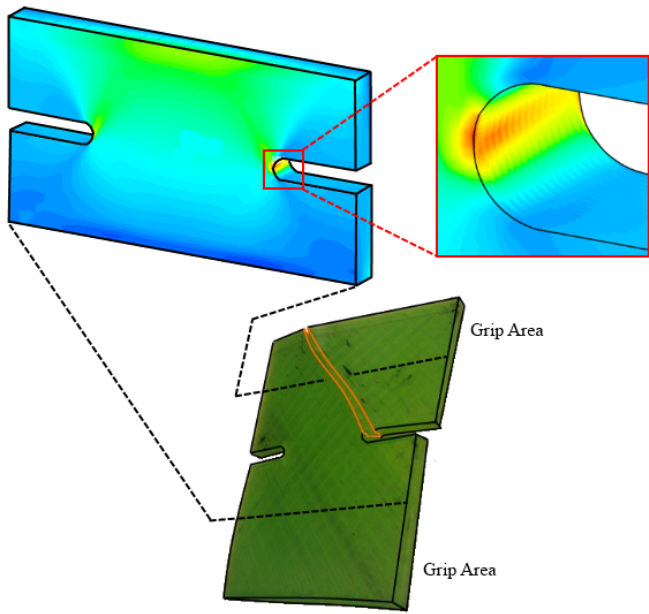


FIGURE 14. FFF test specimen under simulated loading in ANSYS finite-element analysis (top left), with magnified portion showing inter-lamina stress concentrations (top right). A physical test specimen which has failed due to these delamination forces (bottom center) is also shown, with edges and fractures digitally highlighted for clarity.

This theoretical understanding is born out both in the demonstration of Figure 14, and by observations during production. Extrusions within one print layer bond at a relatively high temperature especially due to the rasterized deposition which is typically employed. The temperature is much lower for bonds

between layers, accounting for the poor strength of parts in this direction.

5.2 Mitigating Anisotropic Effects

Given the sources of anisotropy outlined in the previous section, it appears that there are only a few steps that can be taken to improve the mechanical properties of FFF parts in order to enable the manufacture of robust components. These include:

1. printing as slowly as is economical.
2. Extruding the highest temperature possible without degrading surface finish and geometric accuracy.
3. Designing parts to carry axial loads in the plane parallel to the build surface.
4. Designing parts such that moment loads do not induce excessive inter-ply forces.

Of these recommendations, the fourth is most problematic. Due to the high geometric complexity of typical FFF components, computer simulation to determine interplay forces is infeasible for all but the simplest test cases. The application of traditional design methods for orthotropic polymer composites is not appropriate either, as composites are almost never used to construct large solid objects. Additionally, a typical FFF part may consist of thousands of lamina rendering many of the computational techniques for composite design infeasible as well. This indicates that there is a strong need to develop better design tools for the analysis of FFF parts and structures.

6 Future Work and the Path Ahead

The discussion of anisotropy in Section 5 makes it clear that there is a strong need for both better constitutive models of FFF-produced material behaviors, and simulation methods which can be used to predict the performance properties of components manufactured from these materials. The development of these methods will enable the extension of the practices given in Sections 3 and 4. We speculate that a mixed numerical-experimental approach to this problem is appropriate. Given the loose similarity between FFF materials and polymer composites, it may be advantageous to utilize recently developed multiaxial robotic testing techniques [41, 42] as part of this effort. The de-facto choice of finite-element analysis for exploiting these constitutive models should also be carefully considered. In our opinion, a discrete element method [43] or hybrid finite/discrete element method [44] formulation may be more appropriate. These methods offer superior performance in the analysis of discontinuous failure modes (i.e. cracking and delamination) which we have observed to be the dominant modes of failure in FFF components.

There is a great deal of ongoing research into specialized feedstock materials for FFF, such as electrically conductive, ther-

mochromic, or filled/fiber-reinforced filaments. These new products are largely uncharacterized, and require additional study. The development of design guidelines to allow efficient manufacturing using these materials is also necessary. The use of electrically conductive materials may offer an interesting opportunity; if electrical properties are proportional to bond strength, as we might reasonably expect in a diffusion-driven process, then electrical conductance may serve as a useful diagnostic or non-destructive testing technique.

7 Conclusions

This work is an attempt to collect and formalize a great deal of well-known but largely uncommunicated knowledge regarding FFF. In the preceding sections we have provided a broad outline of the FFF process, and enumerated the parameters which govern this process. This led to a presentation of practices which enable efficient and economical production using FFF using low-cost, commonly available 3D printing hardware. These design practices led to a discussion of bulk material properties, and the discussion of how these feedstock materials should be selected and printed. Moving on from bulk properties, we proceeded to the subject of anisotropy, and the role that it plays in FFF technology. The sources of anisotropy were examined, and a numeric/physical experiment illustrated their effect. This examination of anisotropy also illuminates some of the shortcomings of current design methods and tools in a clear light, and we gave our opinions on the best path towards addressing these deficiencies.

By researching and discussing these topics, we present a resource which is of benefit to researchers in the field of manufacturing science, and industrial professionals who are either considering the use of FFF-enabled technologies such as 3D printing, or those who have already entered production and are optimizing their fabrication process. In so doing, we hope to motivate and enable increased effective use of FFF 3D printing for both research and industrial applications. It is clear that this is not a finished effort, and that there is a great deal of future research which is required to fully realize the potential of FFF manufacturing.

ACKNOWLEDGMENT

The authors would like to acknowledge the advice and support of those involved with the Engineering Design Program and Design Innovation and Computational Engineering Laboratory at the Colorado School of Mines in completing this paper. A modified Percent Contribution Indicated (PCI) approach has been used to assign equal contributions to Dr. Cameron J. Turner and Dr. Douglas L. Van Bossuyt as corresponding authors as described within [45].

References

1. C. Chua, K. Leong, and C. Lim, 2010, *Rapid Prototyping: Principles and Applications*, World Scientific Press.
2. M. Frauenfelder, 2012, *Make: Ultimate Guide to 3D Printing*, O'Reiley Media.
3. A. France, 2013, *Make: 3D Printing: The Essential Guide to 3D Printers*, Maker Media Inc.
4. M. Frauenfelder, 2013, *Make: Ultimate Guide to 3D Printing 2014*, Maker Media Inc.
5. B. Wittbrodt, A. Glover, J. Laureto, G. Anzalone, D. Oppliger, J. Irwin, and J. Pearce, 2013, "Life-cycle economic analysis of distributed manufacturing with open-source 3-D printers," *Mechatronics*, 23(6):713-726.
6. J. Pearce, 2012, "Building Research Equipment with Free, Open-Source Hardware," *Science*, 337(6100):1303-1304.
7. M. Agarwala, D. Bourell, J. Beaman, H. Marcus, and J. Barlow, 1995, "Direct selective laser sintering of metals," *Rapid Prototyping Journal*, 1(1):26-36.
8. E. Sachs, M. Cima, P. Williams, D. Brancazio, and J. Cornie, 1992, "Three Dimensional Printing: Rapid Tooling and Prototypes Directly from a CAD Model," *Journal of Manufacturing Science and Engineering*, 114(4):481-488.
9. A. Dolenc and I. Makela, 1994, "Slicing procedures for layered manufacturing techniques," *Computer-Aided Design*, 26(2):119-126.
10. R. Crawford, 1993, "Computer aspects of solid freeform fabrication: geometry, process control, and design," *Proceedings of the 1993 Solid Freeform Fabrication Symposium*, p. 102-111.
11. P. Kulkarni and D. Dutta, 1996, "An accurate slicing procedure for layered manufacturing," *Computer-Aided Design*, 28(9):683-697.
12. P. Pandey, N. Reddy and S. Dhande, 2003, "Real time adaptive slicing for fused deposition modeling," *International Journal of Machine Tools and Manufacture*, 43(1):61-71.
13. S. Singamneni, A. Roychoudhury, O. Diegel and B. Huang, 2012, "Modeling and evaluation of curved layer fused deposition," *Journal of Materials Processing Technology*, 212(1):27-35.
14. B. Huang and S. Singamneni, 2014, "Adaptive slicing and speed- and time-dependent consolidation mechanisms in fused deposition modeling," *Journal of Engineering Manufacture*, doi:10.1177/0954405413497474.
15. P. Cignoni, M. Callieri, M. Corsini, M. Dellepiane, F. Ganovelli, and G. Ranzuglia, 2008, "MeshLab: an Open-Source Mesh Processing Tool," *Proceedings of Eurographics 2008 Italian Chapter Conference*, p. 129-136.
16. B. Evans, 2012, *Practical 3D Printers*, Ch. 4, Apress Publishing.
17. C. Richter and H. Lipson, 2011, "Untethered Hovering Flapping Flight of a 3D-Printed Mechanical Insect," *Artificial Life*, 17(2):73-86.

18. H. Lipson, F. Moon, J. Hai, and C. Paventi, 2004, "3-D Printing the History of Mechanisms," *Journal of Mechanical Design*, 127(5):1029-1033.
19. U. Klammert, U. Gbureck, E. Vorndran, J. Rodiger, P. Meyer-Marcotty, and A. Kubler, 2010, "3D powder printed calcium phosphate implants for reconstruction of cranial and maxillofacial defects," *Journal of Cranio-Maxillofacial Surgery*, 38(8):565-570.
20. L. Shor, M. Gandhi, X. Wen, W. Sun and S. Geri, 2008, "Solid Freeform Fabrication of Polycaprolactone/Hydroxyapatite Tissue Scaffolds," *Journal of Manufacturing Science and Engineering*, 130(2) doi:10.1115/1.2898411.
21. P. Alexander, S. Allen, and D. Dutta, 1998, "Part orientation and build cost determination in layered manufacturing," *Computer Aided Design*, 30(5):343-356.
22. K. Thrimurthulu, P. Pandey and N. Reddy, 2004, "Optimum part deposition orientation in fused deposition modeling," *International Journal of Machine Tools and Manufacture*, 44:585-594.
23. P. Pandey, N. Reddy, and S.G. Dhande, 2007, "Part deposition orientation studies in layered manufacturing," *Journal of Materials Processing Technology*, 185:125-131.
24. H. Byun and K. Lee, 2006, "Determination of the optimal build direction for different rapid prototyping processes using multi-criterion decision making," *Robotics and Computer-Integrated Manufacturing*, 22:69-80.
25. G. Navangul, R. Paul, and S. Anand, 2013, "Error minimization in layered manufacturing parts by stereolithography file modification using a vertex translation algorithm," *Journal of Manufacturing Science and Engineering*, 135(3) doi:0.1115/1.4024035.
26. V. Kumar and D. Dutta, 1997, "An assessment of data formats for layered manufacturing," *Advances in Engineering Software*, 28(3):151-164.
27. Material Data Sheet: "Overview of materials for Acrylonitrile Butadiene Styrene (ABS), Extruded," <http://www.matweb.com>, Accessed April 7, 2014.
28. Material Data Sheet: "Overview of materials for Polylactic Acid (PLA) Biopolymer," <http://www.matweb.com>, Accessed April 8, 2014.
29. Material Data Sheet: "Overview of materials for Polycarbonate, Extruded," <http://www.matweb.com>, Accessed April 7, 2014.
30. Material Data Sheet: "Overview of materials for Polyethylene Terephthalate (PET), Unreinforced," <http://www.matweb.com>, Accessed April 9, 2014.
31. K. Moswen, "FDM Polycarbonate," <http://www.stratasys.com/resources/case-studies/commercial-products/fdm-polycarbonate>, Accessed April 2, 2014.
32. M. Stokes, 2013, *3D Printing for Architects with MakerBot*, Packt Publishing Ltd.
33. S. Hoskins and S. Hoskins, 2014, *3D Printing for Artists, Designers and Makers: Technology Crossing Art and Industry*, Bloomsbury Academic Press.
34. A. Bellini and S. Gucerri, 2003, "Mechanical characterization of parts fabricated using fused deposition modeling," *Rapid Prototyping Journal*, 9(4):252-264.
35. S. Ahn, M. Montero, D. Odell, S. Roundy, and P. Wright, 2002, "Anisotropic material properties of fused deposition modeling ABS," *Rapid Prototyping Journal*, 8(4):248-257.
36. D. Hutmacher, T. Schantz, I. Zein, K. Ng, S. Teoh, and K. Tan, 2001, "Mechanical properties and cell cultural response of polycaprolactone scaffolds designed and fabricated via fused deposition modeling," *Journal of Biomedical Materials Research*, 55(2):203-216.
37. J. Berthelot, 1999, *Composite Materials: Mechanical Behavior and Structural Analysis*, Springer.
38. K. Jud, H. Kausch and J. Williams, 1981, "Fracture mechanics studies of crack healing and welding of polymers," *Journal of Materials Science*, 16:204-210.
39. D. Kline and R. Wool, 2004, "Polymer welding relations investigated by a lap shear joint method," *Polymer Engineering and Science*, 28(1):52-57.
40. X. Zhu, G. Liu, Y. Guo, and Y. Tian, 2007, "Study of PMMA thermal bonding," *Microsystems Technology*, 13:403-407.
41. J. Michopoulos, J. Hermanson, A. Iliopoulos, S. Lambrakos, and T. Furukawa, 2011, "Data-Driven Design Optimization for Composite Material Characterization," *Journal of Computing and Information Science in Engineering*, 11(2):1-10.
42. J. Steuben, J. Michopoulos, A. Iliopoulos, and C. Turner, 2013, "Inverse Characterization of Composite Materials Using Surrogate Models," *Proceedings of the 2013 ASME IDETC/CIE Conferences*.
43. J. Williams, G. Hocking, and G. Mustoe, 1985, "The theoretical basis of the discrete element method," *Proceedings of the 1985 international conference on numerical methods in engineering*.
44. A. Munjiza and D. Owen, 1995, "A combined finite-discrete element method in transient dynamics of fracturing solids," *Engineering Computations*, 12(2):145-174.
45. T. Tschardt, M. Hochberg, T. Rand, V. Resh, and J. Krauss, 2007, "Author Sequence and Credit for Contributions in Multiauthored Publications," *PLoS Biol*, 5(1):e18.